ATLAS NOTE

ATL-PHYS-PUB-2012-001

August 10, 2012

Physics at a High-Luminosity LHC with ATLAS

The ATLAS Collaboration

Abstract

The physics accessible at the high-luminosity phase of the LHC extends well beyond that of the earlier LHC programme. Selected physics goals, spanning from Higgs boson physics to new particle searches and rare top decays, are presented in this document. They illustrate the substantially enhanced physics reach with an increased integrated luminosity of 3000 fb^{-1}, and motivate the planned upgrades of the LHC machine and ATLAS detector.

Disclaimer: This note has been updated in ATL-PHYS-PUB-2012-004. The update supersedes the Higgs section of this note and reports additional studies on vector-boson scattering.

Submitted to *the European Strategy for Particle Physics, Cracow, Poland, 10-12 September 2012*

ATL-PHYS-PUB-2012-001
23/10/2012

Foreword

The ATLAS and CMS Collaborations

CMS and ATLAS have discovered a new Higgs-like boson with a mass of 125-126 GeV. This opens a new chapter in the history of particle physics. In this brief cover note, the main priorities of the ATLAS and CMS Collaborations in this new era are presented. Further adjustments to these priorities may occur as detailed studies of this particle and searches for new physics are extended into new realms at higher energies in future.

The discovery of the new boson was anchored by the final states with the best mass resolution, namely $H\rightarrow\gamma\gamma$ and $H\rightarrow ZZ$ (4e, 4μ or 2e2μ). These modes placed stringent requirements on detector design and performance. Indeed, the ability to search for the SM Higgs boson over the fully allowed mass range played a crucial role in the conceptual design and benchmarking of the experiments and also resulted in excellent sensitivity to a wide array of signals of new physics at the TeV energy scale. Remarkably, the recent discovery came at half the LHC design energy, much more severe pileup, and one-third of the integrated luminosity that was originally judged necessary. This demonstrates the great value of a bold early conceptual design, a systematic programme of development and construction, and a detailed understanding of detector performance, in confronting challenging physics goals.

With data taken in coming years at or near to the design energy of 14 TeV, a broader picture of physics at the TeV scale will emerge with implications for the future of the energy frontier programme. Amongst the essential inputs will be precision measurements of the properties of the Higgs boson and direct searches for new physics that will make significant inroads into new territory. For the foreseeable future the LHC together with CMS and ATLAS will be the only facility able to carry out these studies. This programme is very challenging for the experiments because it requires accurate reconstruction and identification of physics objects (leptons including the τ, heavy flavour tagging, photons, jets, missing transverse energy) from relatively low to very high transverse momenta extending to large rapidity (e.g. to characterise events from vector boson fusion). To retain and extend these capabilities to higher luminosities in the 2020s, existing systems need to be upgraded or replaced. This will require a vision as ambitious as that of the original LHC programme, in particular ensuring that sufficient resources, both financial and human, are made available in a timely fashion; for R&D in the short term, for prototyping in close liaison with industry in the medium term, and further down the line for construction.

To realise the full physics potential of the LHC, we believe it is essential that the High Luminosity (HL-LHC) upgrade to the accelerator be carried out. However, the instantaneous luminosity of $\sim 5\times10^{34}$ $cm^{-2}s^{-1}$ is well beyond design and capabilities of the current experiments. This necessitates upgrades/replacements explicitly targeted towards the broad programme of physics mentioned above. Looking even further ahead, one can foresee scenarios in which a higher energy hadron collider, such as HE-LHC, is critical in making further advances in particle physics. To make this option viable, investment in the R&D and prototyping of high-field dipole magnets must be pursued.

In summary

1. The highest priority in particle physics should be to exploit fully the physics potential of the LHC. To achieve this goal, ATLAS and CMS place the highest priority on securing the resources needed to achieve the following goals:
   - Upgrade/replace selected elements of the apparatus and associated readout, trigger, data acquisition and computing systems in order to exploit fully the phase of LHC running above the original design luminosity over the next 10 years (up to LS3);
   - Prepare, prototype and construct the necessary upgrades/replacements of detectors to operate and optimally exploit the phase of running at instantaneous luminosities of $\sim 5\times10^{34}$ cm^{-2} s^{-1} in the decade following LS3.
2. CMS and ATLAS strongly recommend that resources be allocated for the HL-LHC to enable the LHC to operate at luminosities significantly higher than the original design.
3. ATLAS and CMS strongly support the R&D and prototyping of high-field dipole magnets to provide the capability to build a higher-energy hadron collider in future.

1 Introduction

The LHC is the world's energy frontier collider. At present, its physics programme has just started, with pp collisions at 7 and 8 TeV centre-of-mass energy. The ATLAS and CMS experiments have recently reported the discovery of a new boson with a mass around 126 GeV, consistent with the Standard Model Higgs particle [1, 2]. This marks just the beginning of the physics exploration of the LHC and it opens a new chapter in the study of the mechanism of electroweak symmetry-breaking.

The pp centre-of-mass energy will be increased to close to 14 TeV in 2015 and beyond with a luminosity of $\sim 10^{34}\text{cm}^{-2}\text{s}^{-1}$. Further ahead, an upgrade of the accelerator and detectors to handle luminosities of $\sim 5 \cdot 10^{34}\text{cm}^{-2}\text{s}^{-1}$, foreseen for the early 2020's ("HL-LHC" operation), provides exciting physics opportunities at reasonable cost and the full exploitation of the investment in this project.

The enhanced physics capabilities presented here give a few highlights of the physics case for operation of the LHC at high luminosities. Results are preliminary and will be updated in the coming months. Realistic assumptions have been made regarding the upgraded detector performance at the high pileup foreseen at the HL-LHC, up to 140 events per bunch crossing. The recent observation of a new boson with mass around 126 GeV compatible with the Standard Model Higgs boson opens the road to a wealth of measurements of the new particle. A wide range of other searches have been carried out by ATLAS, extending far beyond previous experiments in sensitivity. To date no evidence has been reported of physics beyond the Standard Model (BSM) in collisions at 7 or 8 TeV, allowing limits to be placed in the TeV range for strongly-produced SUSY particles, and in the range from hundreds of GeV to 2-3 TeV for other new particles. Sensitivity scales rather well with centre-of-mass energy, but the dependence on luminosity is more complex. Some examples are explored in this note. A largely complementary study, however with earlier assumptions on the detector performance, can be found in [3].

The LHC has to date delivered $\sim 5\,\text{fb}^{-1}$ at 7 TeV and $\sim 10\,\text{fb}^{-1}$ at 8 TeV. After the first long shutdown (LS1) in 2013/4 the centre-of-mass energy will increase to 13 – 14 TeV, with luminosities around $10^{34}\text{cm}^{-2}\text{s}^{-1}$. In anticipation of the HL-LHC upgrades, the LHC will install equipment in a one-year shutdown in 2018 (LS2) to allow the instantaneous luminosity to be doubled. An integrated luminosity around $300\,\text{fb}^{-1}$, the goal for the approved LHC programme, should be reached by about 2021. At this point the LHC luminosity can be improved further via the installation of crab cavities, new low-beta insertions, and reduction of the beam emittances. A further one-to-two-year shutdown is foreseen around 2022 (LS3), after which the LHC can be expected to reach luminosities around $5 \cdot 10^{34}\text{cm}^{-2}\text{s}^{-1}$. The ATLAS detector upgrade programme foresees replacement of critical components to allow such operation with a similar detector performance as at present, if necessary with some degree of luminosity-levelling. The total integrated luminosity foreseen for this HL-LHC phase is $3000\,\text{fb}^{-1}$.

2 Higgs boson measurements

After discovering a new Higgs-like boson by ATLAS [1] and CMS [2] a major goal is to establish the nature of this particle by determining the spin/CP quantum numbers and by increasingly precise measurements of couplings to fermions and vector bosons. A Standard Model Higgs boson with mass 126 GeV is particular suited for studies at the LHC since it decays to many final states that can be experimentally reconstructed.

Models with an extended Higgs sector, like Supersymmetry, predict deviations of the Higgs couplings from Standard Model predictions that can be large, but can also be arbitrarily small, e.g. in Supersymmetry, when the other Higgs states are very heavy. The goal is therefore to measure couplings as precisely as possible and in parallel look for other (heavier) particles of the spectrum of the new theory.

For a final confirmation of the Higgs mechanism an observation and measurement of the triple (and quartic) Higgs self-coupling is important. While the quartic Higgs boson coupling is not accessible

within any currently planned collider, the triple Higgs coupling could be observable as an interference effect in the Higgs boson pair production.

In the following, we assume that the recently discovered particle is the Standard Model Higgs boson and study the precision with which its properties can be measured for some selected cases with the luminosity upgrade of the LHC.

2.1 Measurement of the spin/CP nature

From the present observations it is known that the new particle must be a boson and, since it is observed in the $\gamma\gamma$ final state it cannot have spin 1.[1] If the new particle is assumed to be a pure state its spin/CP quantum numbers can be measured to some extent already with $\sim 30\,\text{fb}^{-1}$ that should be collected during the present 8 TeV running phase of the LHC. Study of the $H \to ZZ^* \to 4l$ decay can exclude 0^- and 1^- CP states with more than $2\,\sigma$ while the separation from the other states is weaker. A combination with $H \to WW^*$ and $H \to \gamma\gamma$ channels will provide a better separation between spin-1 and spin-2 hypotheses. With $300\,\text{fb}^{-1}$ at 14 TeV the spin/CP quantum numbers of non-mixed states can finally be established with a significance of more than $5\,\sigma$. For a mixed states the possible precision on the mixing angle is currently under study.

2.2 Measurements of the Higgs boson couplings

While measurements will begin within the approved LHC programme, the luminosity of the HL-LHC will provide substantially improved statistical precision for already established channels and allow to study rare Higgs boson production and decay modes. From the combination of the observed rates in all channels, detailed measurements of the Higgs boson coupling strength can then be extracted.

For an estimate of the precision with which the SM Higgs boson couplings to other particles can be measured at the HL-LHC, the following Higgs boson decays, that are already addressed in the current 7 and 8 TeV analysis, are considered:

- $H \to \gamma\gamma$ in the 0-jet and the 2-jet final state with a vector-boson fusion (VBF) selection. The analysis is carried out analogously to Ref. [1].
- Inclusive $H \to ZZ^* \to 4\ell$ following a selection close to that in Ref. [1].
- $H \to WW^* \to \ell\nu\,\ell\nu$ in the 0-jet and the 2-jet final state with a VBF selection following closely that of Ref. [1].
- $H \to \tau^+\tau^-$ in the 2-jet final state with a VBF selection as in Ref. [4].

For all channels, changes to the trigger and the photon/lepton selections needed to keep misidentification rates at an acceptable level at high luminosities are taken into account. For the VBF jet selection, the cuts were tightened to reduce the expected fake rate from pileup to be below 1% of the jet activity from background processes.

In addition to these channels, two additional channels targeted at the measurement of fermion couplings with high luminosities have been studied:

- $t\bar{t}H, H \to \gamma\gamma$: this channel has a very low signal rate at the LHC, but one can expect to observe more than 100 events with the HL-LHC. The selection of the diphoton system is done in the same way as for the standard $H \to \gamma\gamma$ channel. In addition, a 1-lepton selection with a cut on the scalar sum H_T of all jet transverse momenta and a 2-lepton selection with a Z-veto are applied in order to

[1] We are aware that there are exotic models allowing the new particles to decay into two very light pseudoscalar particles that subsequently decay into two almost overlapping photons each.

enhance the $t\bar{t}H, H \to \gamma\gamma$ signal. The $t\bar{t}H$ initial state yields a precise measurement of the square of the top-Yukawa coupling. Figure 1(a) shows the expected signal in the 1-lepton final state and Fig 2(a) shows the expected measurement precision for both considered final states.

- Inclusive $H \to \mu\mu$: this channel has also a low signal rate at the LHC with a signal-to-background ratio of only $\sim 0.2\%$. However, the expected narrow signal peak allows a signal extraction at very high luminosities, resulting in an expected signal significance larger than $6\,\sigma$ with $3000\,\text{fb}^{-1}$. The analysis follows Ref. [5] with changes to maximise the sensitivity for an inclusive $\mu\mu$ signal. Fig. 1(b) shows the expected signal compared to the large continuous background and Fig 2(a) shows the expected measurement precision.

An overview of the expected measurement precision on the signal rate in each channel is given in Fig. 2(a) for assumed integrated luminosities of $300\,\text{fb}^{-1}$ and $3000\,\text{fb}^{-1}$. The $\gamma\gamma$ and ZZ^* final states profit most from the high luminosity, as both statistical and systematic uncertainties (which are dominated by the number of events in the sideband) are reduced considerably. The $b\bar{b}$ final state is not yet included in these estimates, as both jet energy resolution and b-tagging suffer from the high luminosity conditions and need careful studies with a realistic and well understood upgrade detector design. For the WW^* channels the signal rate is not the limiting factor, and background systematic uncertainties rapidly become dominant. However, the addition of some rare channels with clean final state signatures, like WH or ZH with $H \to WW$, ZZ, $\gamma\gamma$, is expected to improve the overall results considerably and yield precise measurements of W-coupling related processes. These channels are subject to further studies.

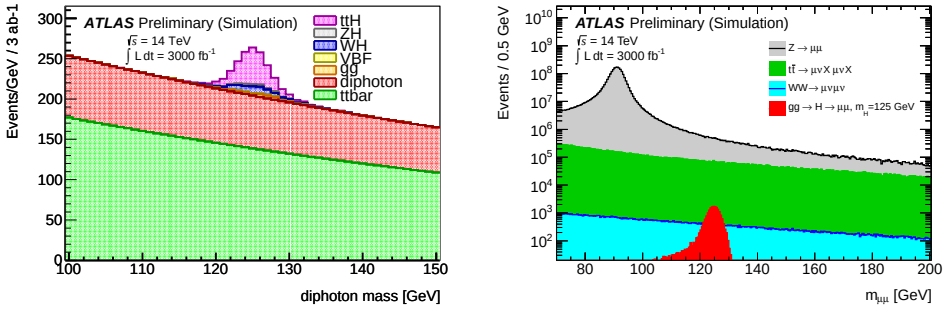

(a) (b)

Figure 1: Expected invariant mass distribution for (a) $t\bar{t}H, H \to \gamma\gamma$ in the 1-lepton selection and (b) the inclusive $H \to \mu\mu$ channel, for an assumed integrated luminosity of $3000\,\text{fb}^{-1}$

All measurements are combined in a general coupling fit, where no assumption about the particle content of the $H \to \gamma\gamma$ and $gg \to H$ loops is made. Furthermore, no assumption on possible BSM Higgs boson decay modes and hence on the total width Γ_H is made, which allows only the measurement of ratios of coupling parameters. For a given production mode i and decay channel j the cross section $\sigma_i \cdot \text{BR}_j$ is assumed to be proportional to $\Gamma_i \cdot \Gamma_j / \Gamma_H$ with $i = g, W, Z, t$ and $j = W, Z, \gamma, \mu, \tau$. The coupling fit parameters are chosen as the ratios

$$\frac{\Gamma_W}{\Gamma_Z}, \frac{\Gamma_\gamma}{\Gamma_Z}, \frac{\Gamma_\tau}{\Gamma_Z}, \frac{\Gamma_\mu}{\Gamma_Z}, \frac{\Gamma_t}{\Gamma_g}, \frac{\Gamma_Z}{\Gamma_g} \text{ and } \frac{\Gamma_g \cdot \Gamma_Z}{\Gamma_H} \,. \tag{1}$$

Figure2(b) shows the expected uncertainties on the determination of these coupling parameters assuming an integrated luminosity of $300\,\text{fb}^{-1}$ and $3000\,\text{fb}^{-1}$. The experimental uncertainties are reduced by a factor of two or more for almost all ratios with $3000\,\text{fb}^{-1}$ compared to $300\,\text{fb}^{-1}$ and reach $\sim$5% for the

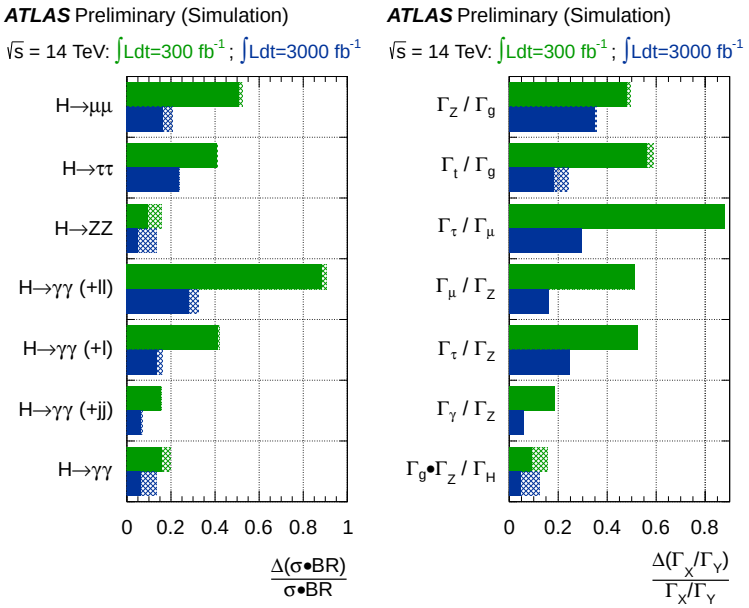

(a) (b)

Figure 2: (a): Expected measurement precision on the signal strength in all considered channels for luminosities of 300 fb^{-1} and 3000 fb^{-1}. (b): Expected measurement precisions on ratios of Higgs boson partial widths without theory assumptions on the particle content in Higgs loops or the total width.The bars give the expected uncertainty on the signal cross sections (the dashed areas include current theory uncertainties from scale and PDF variations).

best cases. The ratios Γ_γ/Γ_Z and Γ_t/Γ_g provide constraints on new physics contributions to the $H \to \gamma\gamma$ and $gg \to H$ loops at the ~5–20% level. For the derived ratio Γ_τ/Γ_μ, that gives insight into the coupling relation between the 2$^{\text{nd}}$ and 3$^{\text{rd}}$ fermion generation, a precision of ~30% is reachable.

In a minimal coupling fit, where only two independent scale factors C_V and C_F for the vector and fermion couplings and no additional BSM contributions are allowed in loops or in the total width ($\sigma_{V,F} \sim \Gamma_{C,F} \sim C^2_{V,F}$), experimental precisions of ~5% on C^2_V and ~7% on C^2_F are expected with 3000 fb^{-1} (~10% and ~15% with current theory cross section uncertainties), a reduction of about a factor of two compared to 300 fb^{-1}.

2.3 Observation of the Higgs self coupling

In order to completely determine the parameters of the Standard Model and establish the Higgs mechanism as being responsible for the electroweak symmetry breaking, the measurement of the Higgs self-couplings and subsequent reconstruction of the Higgs potential is important. A direct analysis of the Higgs boson trilinear self-coupling λ_{HHH} can be done via the detection of Higgs boson pair production. At hadron colliders, the dominant production mechanism is gluon-gluon fusion, and for centre-of-mass energies of 14 TeV, the production cross section of two 125 GeV Higgs bosons is estimated[2] to be 34 fb. Due to the destructive interference of diagrams involving $gg \to HH$, the cross section is enhanced at lower values of λ_{HHH}; cross sections for $\lambda_{HHH}/\lambda^{SM}_{HHH} = 0$ and $\lambda_{HHH}/\lambda^{SM}_{HHH} = 2$ are $\sigma_{\lambda=0} = 71$ and $\sigma_{\lambda=2} = 16$ fb respectively.

A Higgs boson mass $m_H \approx 125$ GeV implies a number of potential channels to investigate, due to a

[2]Cross sections at NLO calculated using the HPAIR package [6].

wide spectrum of decay modes. Sensitivity studies at the generator level[3] for the HL-LHC upgrade were performed on just two channels, $HH \to b\bar{b}\gamma\gamma$ and $HH \to b\bar{b}W^+W^-$, chosen for their clean signature and high branching ratio, respectively[4].

2.3.1 $HH \to b\bar{b}W^+W^-$ channel

The branching ratio of the $HH \to b\bar{b}W^+W^-$ channel is 25%, which results in 25k expected events in 3000 fb^{-1} at 14 TeV including all possible W boson decay modes. However the final state is identical to $t\bar{t}$-production giving a huge potential background to this decay mode. For this study the semi-leptonic channel, where one W boson decays hadronically and the second one leptonically, is chosen.

Events are selected if they contain exactly one lepton, at least four jets with at least one of them b-tagged and missing transverse momentum. The W- and the Higgs bosons are reconstructed using a χ^2 fitting-technique and events are selected if the masses of the WW- and $b\bar{b}$-systems are close to the Higgs boson mass.

The signal to background ratio before cuts is of the order of 10^{-5}, consistent with the results of Ref. [7]. The analysis cuts reduce the background to the percent level but also effect the signal efficiency so that no constraints on the Higgs self-coupling can be obtained from this channel.

2.3.2 $HH \to b\bar{b}\gamma\gamma$ channel

The $HH \to b\bar{b}\gamma\gamma$ channel has a branching ratio of 0.27%, resulting in a predicted yield of 260 events in 3000 fb^{-1} of 14 TeV pp collisions. Three main backgrounds are considered; the irreducible $\gamma\gamma b\bar{b}$, $b\bar{b}H(H \to \gamma\gamma)$ and $t\bar{t}H(H \to \gamma\gamma)$, which have $\sigma \times BR$ of 111, 0.124 and 1.71 fb respectively, compared to 0.087 fb for the signal.

The energies of the final state particles and jets are smeared based on a parameterisation extrapolated to the upgraded detector and high luminosity pileup. For photons, a smearing of the direction is also applied. The expected photon identification efficiency is around 80% and the b-tagging efficiency of between 70 and 80%.

Events are selected that contain two b-jets and two photons with $50 < M_{b\bar{b}} < 130$ GeV and $120 < M_{\gamma\gamma} < 130$ GeV respectively, where the following object definitions are used. For b-jets: b-tagged and $p_T > 40/25$ GeV for the leading/sub-leading jet. For photons: p_T >25 GeV, and fulfilling an isolation requirement. Additionally, cuts are applied on the angles between $b-b$, $\gamma-\gamma$ and $b-\gamma$ pairs, based on those described in [8]. Finally, a lepton veto and a jet multiplicity cut are applied.

Following this selection, a signal yield of approximately 12 events is obtained, with the irreducible $\gamma\gamma b\bar{b}$ background sample of more than 300,000 events completely suppressed and the $b\bar{b}H$ contribution to a negligible level. The only significant background remaining is $t\bar{t}H$, contributing approximately 18 events. This corresponds to a S/B ratio of around 0.7 ($\frac{S}{\sqrt{B}} = 2.8$).

In addition to the SM value $\lambda_{HHH} = 1$, the study was repeated using signal samples with $\lambda_{HHH} = 0$ and $\lambda_{HHH} = 2$. Yields of approximately 18 and 6 events were obtained for the $\lambda_{HHH} = 0$ and $\lambda_{HHH} = 2$ cases respectively. With this decay mode alone first evidence of double-Higgs boson production can be obtained but the Higgs self-coupling cannot be established. However with the addition of a few other decay modes with similar significance some constraints on λ_{HHH} should be possible.

2.3.3 Summary on Higgs self-coupling studies

Preliminary studies of the $HH \to b\bar{b}\gamma\gamma$ channel show that a sensitivity for double Higgs boson production of $\sim 3\sigma$ per experiment is within reach. Additional channels such as $HH \to b\bar{b}\tau^+\tau^-$, the subject of

[3] Event files produced by Dolan, Englert and Spannowsky as described in [7].

[4] The $b\bar{b}b\bar{b}$ final state has the highest branching ratio, but is expected to be too difficult to extract from the huge background

a promising recent phenomenological study [7], are under investigation. By adding more channels and combining both experiments a $\sim 30\%$ measurement of λ_{HHH} may be achieved. Further studies will be made in the coming months to consolidate and expand this projection.

3 Weak boson scattering

The exploration of physics at the TeV scale is the major goal of the LHC, and many extensions of the SM involve anomalous quartic couplings. The luminosity upgrade of the LHC can have a major impact in discovering an extended electroweak symmetry-breaking sector beyond the SM Higgs mechanism [3]. In this section we discuss the sensitivity of ATLAS to WW scattering using as a reference model the PYTHIA implementation of the electroweak chiral Lagrangian with unitarised amplitudes for WW scattering [9]. In this model, unitarisation is implemented using the Inverse Amplitude Method, also known as the Pade Method. Other unitarisation schemes for this Lagrangian have also been discussed in the literature [10].

Experimentally, a striking feature of vector boson scattering is the presence of two high-p_T jets in the forward-backward regions, similar to those found in Higgs vector boson fusion production. The absence of colour exchange in the hard scattering process leads to rapidity gaps in the central part of the detector, however the gap topology will be difficult to exploit due to the high level of pileup. In the semi-leptonic channel two high-energy jets are required, one in each of the forward and backward regions, with large dijet invariant mass, and only one large-radius jet in the central region, from the hadronic decay of the boosted W boson. A high-p_T lepton and large missing transverse energy are also required, a consequence of the leptonic decay of the second W boson. The main backgrounds arise from top pair decays and W + jet final states.

Vector boson scattering can be parameterised by an effective chiral Lagrangian. There are two new operators that are not visible in oblique corrections or triple gauge couplings and conserve the custodial $SU(2)$ symmetry that is suggested by the ρ parameter being close to one. These two operators are scaled by numerical coefficients a_4 and a_5. If the 126 GeV particle discovered at the LHC is confirmed to be the SM Higgs boson, the SM predicts that unitarity of scattering amplitudes in longitudinal vector boson scattering will be maintained at high energy. It is important to confirm this prediction experimentally. Alternate models such as Technicolour and little Higgs have been postulated which encompass TeV-scale resonances and a light scalar particle. Other mechanisms for enhancing vector boson scattering at high energy are possible, even after the SM Higgs boson is established. To maintain generality and to enable comparisons with other studies [11, 12, 13], we use the a_4 and a_5 parameters with unitarised amplitudes to compare sensitivities at different integrated luminosities.

In the following, we show the results of two analyses: In the semileptonic channel $pp \to WW+2j \to l\nu + 4j$ and $pp \to WW + 2j \to e\nu\mu\nu + 2j$. The first channel has more background, but allows a full kinematic reconstruction of the invariant mass of the system that originated the WW final state, while in the cleaner dileptonic decay mode this mass cannot be measured. The lepton+jets channel is therefore more suited for observing resonances directly, while the dilepton channel is used to explore sensitivity via enhancement of the rate of high-p_T leptons from the WW scattering.

The dilepton channel is relatively free of mis-identification backgrounds from W+jets and QCD multi-jet processes. In this study we use the $e\mu$ channel which is also free from the Z+jets background. We protect against jet mis-identification backgrounds by requiring the tagging jets to have $p_T > 50$ GeV. The dominant background is from $t\bar{t}$ production, followed by diboson production.

The sensitivity to new physics in vector boson scattering depends on jet, lepton and missing energy reconstruction in a high-pileup regime. Fully simulated events under high-pileup conditions have been produced, and efficiencies and resolutions have been estimated for the various objects. These quantities have been used to smear particle-level outputs for various new-physics scenarios. The $WW/WZ \to \ell\nu jj$

channel places the most stringent requirements on the single-lepton triggers, but we assume that triggers combining high-p_T leptons, jets and missing transverse energy will not be pre-scaled.

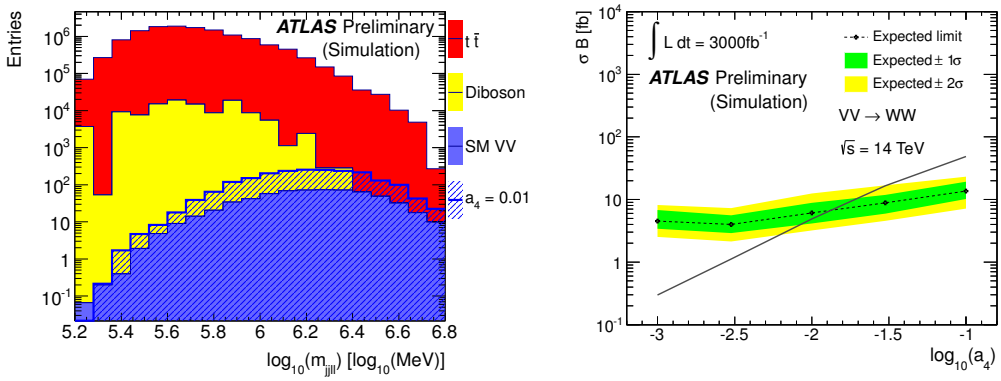

Figure 3: The reconstructed 4-body mass spectrum using the two leading leptons and jets for WW scattering in the $pp \to WW + 2j \to e\nu\mu\nu + 2j$ channel, showing backgrounds and signal for a value of $a_4 = 0.01$ (left), and the limit that can be set on the a_4 parameter (right) using the experimental σB limit (band) and the predicted cross section as a function of a_4 (solid line) for this channel.

Table 1: Summary of expected upper limits for a_4 at the 95% confidence level using the $pp \to WW + 2j \to e\nu\mu\nu + 2j$ search at $\sqrt{s} = 14$ TeV in the absence of a signal.

model	300 fb^{-1}	1000 fb^{-1}	3000 fb^{-1}
a_4	0.066	0.025	0.016

Figure 3 shows the 4-body ($\ell\ell jj$) mass spectrum reconstructed in the fully-leptonic decay mode using the two leading leptons and jets for an integrated luminosity of 3000 fb^{-1}, as well as the expected limits on the cross section times branching ratio (σB) as a function of the a_4 parameter. Comparing to the predicted σB (theory curve shown), the expected limit on a_4 from the dileptonic decay mode is summarised in Table 1. The theoretical σB is taken as the difference between the prediction at a given value of a_4 and the prediction at $a_4 = 0$. The increase of a factor of ten in integrated luminosity makes ATLAS sensitive to a_4 values smaller by a factor of four, allowing ATLAS to probe $a_4 \sim 1\%$. The effective Lagrangian parameters in the range $10^{-3} - 10^{-2}$ are compatible with precision electroweak constraints. Thus, the high-luminosity LHC allows us to probe this interesting range of parameter space.

In the semi-leptonic channel, the forward jets are required to have $p_T > 40$ GeV, pseudo-rapidity $|\eta| > 1.5$ and to be in opposite hemispheres. The central jet in the event, identified as the hadronically-decaying boosted W boson, is reconstructed using the same algorithm as the forward jets. It is required to have $p_T > 300$ GeV and have jet mass between 60 and 110 GeV. The lepton is required to have $p_T > 60$ GeV and large missing transverse momentum is also required. The leptonically-decaying W boson is required to have $p_T^W > 200$ GeV. Finally, a top quark veto is applied which consists of combining all jets with the central jet and extracting the invariant mass for each combination. Events are discarded if one dijet combination gives a mass close to the top quark mass (lies within the range [140, 240] GeV).

Figure 4 shows the reconstructed WW invariant mass in the semi-leptonic channel. The dominant backgrounds are compared to resonance hypotheses obtained from the generalised chiral Lagrangian model; the resonance pole masses are listed in Table 2 and have a predicted width of $O(100$ GeV), as determined by the (a_4, a_5) values given in the table.

As shown in this figure, the background is dominated by $t\bar{t}$ and diboson events. The $W + 3$ jets and $W + 4$ jets backgrounds are not significant.

Table 2: Summary of sensitivity to various resonance hypotheses in the semi-leptonic WW channel.

model	baseline	500 GeV scalar	800 GeV vector	1150 GeVvector
(a_4, a_5)	$(0, 0)$	$(0.01, 0.009)$	$(0.009, -0.007)$	$(0.004, -0.004)$
S/B	$(3.3 \pm 0.3)\%$	$(0.7 \pm 0.1)\%$	$(4.9 \pm 0.3)\%$	$(5.8 \pm 0.3)\%$
$S/\sqrt{B}$ $(L = 300\text{fb}^{-1})$	2.3 ± 0.3	0.6 ± 0.1	3.3 ± 0.4	3.9 ± 0.4
$S/\sqrt{B}$ $(L = 3000\,\text{fb}^{-1})$	7.2 ± 0.1	1.6 ± 0.1	10.4 ± 0.7	12.4 ± 0.7

Quoted in Table 2 is the significance of the resonant excess over background for integrated luminosity of 300 fb^{-1} and 3000fb^{-1}. These numbers illustrate the discovery potential for a new vector resonance of mass ~1 TeV, which is an interesting mass range to probe in the context of electroweak symmetry-breaking. The increase by a factor of ten in integrated luminosity enables these searches to cross the discovery threshold.

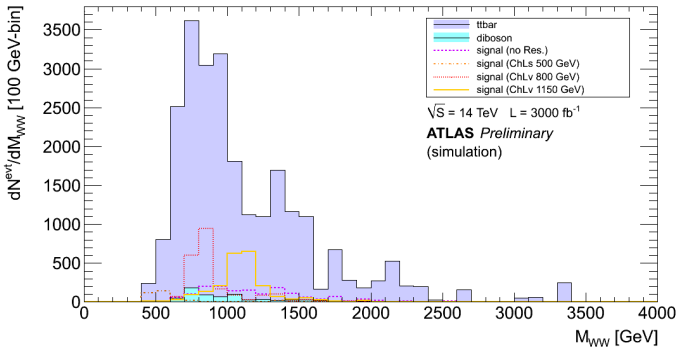

Figure 4: The reconstructed invariant mass spectrum of the WW system in the semi-leptonic channel with 3000fb^{-1}, for $t\bar{t}$ and diboson SM backgrounds as well as signals with various resonant masses; the choice of parameters in the chiral Lagrangian model is given in the text.

4 Supersymmetry searches and measurements

The discovery (or exclusion) of weak scale supersymmetry (SUSY) remains among the highest priorities for the LHC experiments. By introducing supersymmetric partners to all SM particles, SUSY removes the quadratic divergences that accompany a fundamental scalar Higgs boson. In the framework of generic R-parity conserving supersymmetric extensions of the SM, SUSY particles are produced in pairs and the lightest supersymmetric particle (LSP) is stable. The LSP provides the massive thermal relic required to explain the cosmological dark matter. The lightest neutralino is often assumed as LSP, where neutralinos ($\tilde{\chi}^0_j$, $j = 1, 2, 3, 4$) and charginos ($\tilde{\chi}^\pm_i$, $i = 1, 2$) are the mass eigenstates originating from the mixture of the SUSY partners of Higgs and electroweak gauge bosons (higgsinos and gauginos). The scalar partners of right-handed and left-handed fermions can mix to form two mass eigenstates, nearly degenerate in case of first and second generation squarks and sleptons ($\tilde{q}$ and $\tilde{l}$), whilst possibly split in case of bottom and top squarks (sbottom, $\tilde{b}$ and stop, $\tilde{t}$) and tau sleptons (stau, $\tilde{\tau}$). The lighter stop mass eigenstate can thus be significantly lighter than the other squarks and the gluinos ($\tilde{g}$, supersymmetric partners of the gluons). The world-leading constraints on the masses of many supersymmetric particles arise from the ATLAS and CMS experiments at $\sqrt{s} = 7$ TeV and 8 TeV. Assuming a light LSP, the 1st and 2nd generation squark and gluino masses are currently excluded below about 1.4 TeV and 1.0 TeV, respectively [14]. Less stringent limits are placed on third generation squarks [15], gauginos [16] and sleptons (superpartners

of leptons), where the mass constraints strongly depends on the assumed SUSY mass spectrum [16, 17]. The sensitivity to heavy SUSY particles will be increased significantly when the full LHC energy of $\sqrt{s} = 14\,\text{TeV}$ is reached. In the following, the improvement in mass reach comparing $300\,\text{fb}^{-1}$ to $3000\,\text{fb}^{-1}$ is discussed for three types of SUSY searches, inspired by simplified standard analyses developed for 7 and 8 TeV data. Coarse systematic uncertainties of 30% on the background estimates are assumed to determine the reach. The sensitivity is expressed in terms of expected 5σ discovery reach and exclusion limits at 95% CL.

Squark and gluino searches Generic searches for the production of squarks of the first two generations and gluinos are carried out in events with final states characterised by the presence of multiple jets and large missing transverse momentum. Figure 5(a) shows the discovery potential and exclusion reach achievable for $\tilde{q}$ and $\tilde{g}$ in an illustrative simplified model with a massless LSP. An increase of integrated luminosity from $300\,\text{fb}^{-1}$ to $3000\,\text{fb}^{-1}$ improves the sensitivity to both particles by approximately 400-500 GeV, a result confirmed in independent studies [19]. These results remain essentially unchanged for LSP masses up to about 1/3 of the mass of the strongly produced particle. If large deviations are observed with respect to the SM background estimates, dominated by $Z \to \nu\nu$+jets and $t\bar{t}$ production, the kinematic properties of the events can be studied and decay products in the decay chain of the SUSY particles can be identified. Figure 5(b) shows the m_{bb} invariant mass distribution for a benchmark SUSY model with squarks and gluinos decaying in complex final states including Higgs bosons, for which with $3000\,\text{fb}^{-1}$ the SUSY Higgs signal yield could be determined to ≈10%.

Third generation searches Naturalness arguments [20, 21] require the top squark to be light, typically below 1 TeV. At $\sqrt{s} = 14\,\text{TeV}$ the direct stop pair production cross section for 600 GeV (1 TeV) stops is 240 (10) fb. An increase in luminosity from $300\,\text{fb}^{-1}$ to $3000\,\text{fb}^{-1}$ increases the sensitivity to heavy stop or, if stop candidates are found, will allow to measure their properties. Stops can decay in a variety of modes which typically includes top or b-quarks, W/Z or Higgs bosons, and an LSP. Pair production signatures are thus characterised by the presence of several jets, including b-jets, large missing transverse

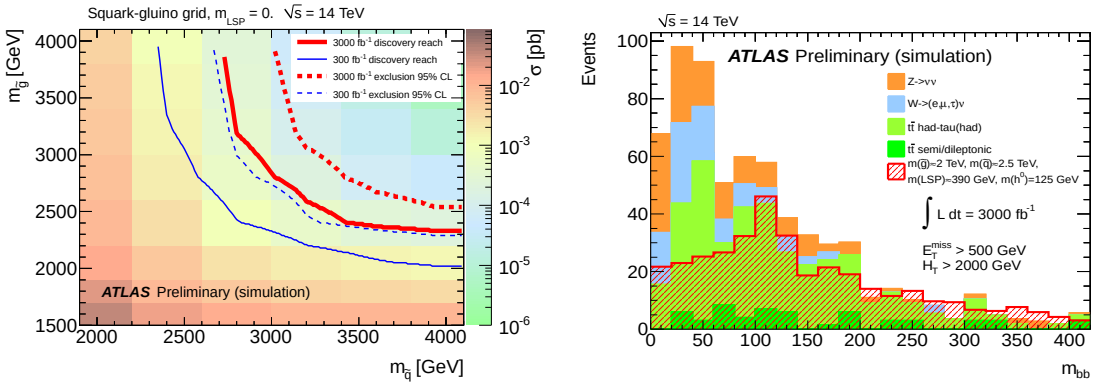

(a) (b)

Figure 5: (a) The 95% CL exclusion limits (solid lines) and 5σ discovery reach (dashed lines) in a simplified squark–gluino model with massless neutralino with $300\,\text{fb}^{-1}$ (blue lines) and $3000\,\text{fb}^{-1}$ (red lines). The colour scale shows the $\sqrt{s} = 14\,\text{TeV}$ NLO production cross section calculated by `Prospino 2.1` [18]. (b) The m_{bb} invariant mass distribution for a benchmark SUSY model compared to the SM background processes for $3000\,\text{fb}^{-1}$ of integrated luminosity.

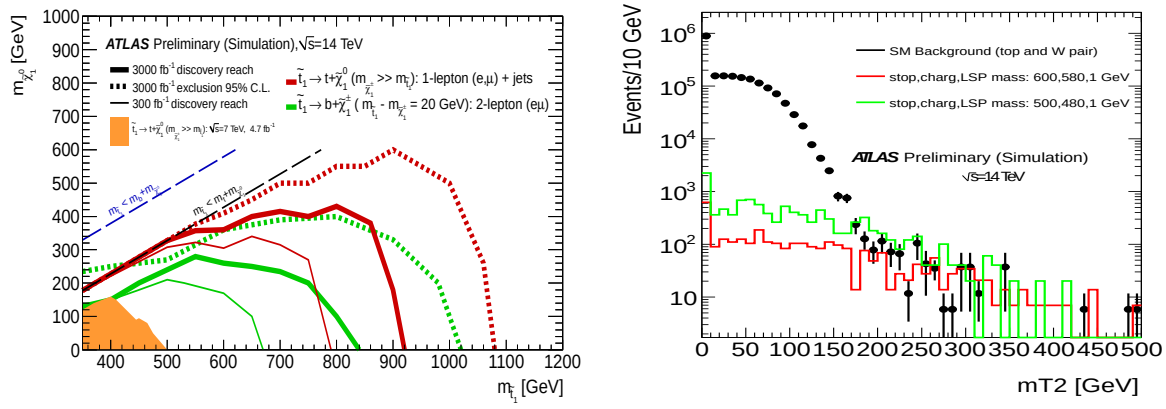

(a) (b)

Figure 6: (a) The 95% CL exclusion limits for 3000 fb^{-1} (dashed) and 5σ discovery reach (solid) for 300 fb^{-1} and 3000 fb^{-1} in the $\tilde{t}, \tilde{\chi}_1^0$ mass plane assuming the $\tilde{t} \to t + \tilde{\chi}_1^0$ (red) or the $\tilde{t} \to b + \tilde{\chi}_1^\pm, \tilde{\chi}_1^\pm \to W + \tilde{\chi}_1^0$ (green) decay mode. (b) The m_{T2} distribution for two-lepton channel for SM background and 2 benchmark SUSY scenarios.

momentum and possibly leptons. Two studies are carried out targeting different decay modes and based on standard counting analyses. A one-lepton-based selection ($\ell \in \{e, \mu\}$) with stringent requirements on missing transverse momentum is employed to search for $\tilde{t} \to t + \tilde{\chi}_1^0$; in this case, the main SM background arises from $t\bar{t}$ production. A two-lepton-based selection ($e\mu$ only) is used for scenarios with $\tilde{t} \to b + \tilde{\chi}_1^\pm, \tilde{\chi}_1^\pm \to W^\pm + \tilde{\chi}_1^0$, where the dilepton m_{T2} [22, 23] variable is taken as the main discriminant against SM background processes dominated by top and W pair production. Figure 6(a) shows the discovery and exclusion potential versus the $\tilde{t}$ and $\tilde{\chi}_1^0$ masses in the two studies. The m_{T2} distribution for the two-lepton channel, useful to distinguish the SUSY signal from SM background processes, is shown in Fig. 6(b). A ten-fold increase in integrated luminosity increases the sensitive stop mass range by up to 200 GeV. Further improvements in analyses techniques exploiting specific features that differentiate signal from SM background (*i.e.* missing transverse momentum shape, angular correlations, boosted objects) and taking into account additional final states can considerably extend the mass reach especially in case of heavy $\tilde{\chi}_1^0$.

Electroweak Gaugino searches Based also on naturalness arguments the $\tilde{\chi}_1^\pm$ and $\tilde{\chi}_j^0$ ($j = 1, 2$) are expected to have masses in the hundreds of GeV range [20, 21] and potentially be within the reach of the LHC. In scenarios with heavy squarks and gluinos, direct pair production of weak gauginos (and/or sleptons) dominates the SUSY production at the LHC. The cross-section of $\tilde{\chi}_1^\pm$-$\tilde{\chi}_2^0$ associated production ranges from 10 to 10^{-2} pb for masses between 50 and 600 GeV. The $\tilde{\chi}_1^\pm$ can decay as $\tilde{\chi}_1^\pm \to W^{\pm(*)}\tilde{\chi}_1^0$ whereas the $\tilde{\chi}_2^0$ as $\tilde{\chi}_2^0 \to Z^{(*)}\tilde{\chi}_1^0$, leading to final states with three leptons and missing transverse momentum where a pair of same-flavour and opposite-sign leptons has a mass consistent with that of a Z boson. In the analysis, a BR($\tilde{\chi}_1^\pm\tilde{\chi}_2^0 \to W^{(*)}\tilde{\chi}_1^0 Z^{(*)}\tilde{\chi}_1^0$) of 100% is assumed. The search is optimised using several kinematic variables to discriminate the signal from the two dominant background processes, namely top-pair and WZ production. With an integrated luminosity of 300 fb^{-1}, scenarios with chargino masses up to 250 GeV can be probed for $\tilde{\chi}_1^0$ mass values below 100 GeV. With a ten-fold increase in luminosity, the discovery potential is extended to scenarios with chargino masses values of ~800 GeV and $\tilde{\chi}_1^0$ masses below ~300 GeV (see Figure 7(a)). Figure 7(b) shows the missing transverse momentum for the

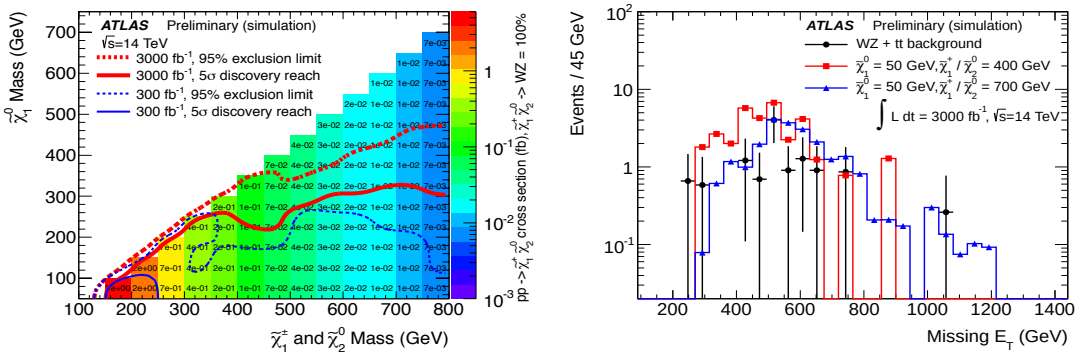

(a) (b)

Figure 7: (a) The 95% CL exclusion limits (dashed lines) and 5σ discovery reach (solid lines) for charginos and neutralinos undergoing $\tilde{\chi}_1^\pm\tilde{\chi}_2^0 \rightarrow W^{(*)}\tilde{\chi}_1^0 Z^{(*)}\tilde{\chi}_1^0$ decays with BR=100%. The case of 300 fb^{-1} and 3000 fb^{-1} are reported. (b) The missing transverse momentum distribution in three-lepton events surviving the BDT-based selection.

SM background and two benchmark SUSY points for three lepton events surviving the final selection. Independent studies [19] show that for processes like $pp \rightarrow \tilde{\chi}_2^0+\tilde{\chi}_1^\pm \rightarrow (h\tilde{\chi}_1^0) + (W^\pm\tilde{\chi}_1^0)$, the ten-fold luminosity increase more than doubles the sensitivity to W-ino masses, from 450 GeV to 950 GeV.

SUSY summary The sensitivity to heavy SUSY particles will be increased significantly when the full LHC energy of $\sqrt{s} = 14$ TeV is reached. An increase of integrated luminosity from 300 fb^{-1} to 3000 fb^{-1} improves the sensitivity to first and second generation squarks and gluinos by approximately 400-500 GeV, and to stops by about 200 GeV. The discovery potential for associated production of charginos and neutralinos extends to scenarios with chargino masses of ~800 GeV for $\tilde{\chi}_1^0$ masses below ~300 GeV. With the data from the high luminosity phase, ATLAS will either find signals for SUSY or it will show that weak-scale SUSY has a poor claim to being the solution to the fine tuning and other problems of the SM. If evidence for new particles is found with 300 fb^{-1} of $\sqrt{s} = 14$ TeV data, dedicated analyses with a 3000 fb^{-1} dataset will provide complementary information about the mass, spin and couplings of the SUSY particles.

5 Exotics

The luminosity upgrade of the LHC substantially increases its potential for discovery and study of exotic new phenomena [3]. While the range of models and their respective parameters is quite large, their salient feature is the production of high-p_T leptons, photons, jets and missing E_T. Our goal is to ensure that the detector design maintains the sensitivity to any signature containing these characteristics. In this section we discuss two benchmark models of new physics and the expected gain in sensitivity if the ATLAS dataset were increased from 300 fb^{-1} to 1000 fb^{-1} and 3000 fb^{-1} at $\sqrt{s} = 14$ TeV.

In order to characterise the high-mass reach we consider resonances with different production and decay mechanisms. As an example of strongly-produced, wide resonances we consider the Kaluza-Klein (KK) gluons g_{KK} in extra-dimensional models [24]. Many signatures of new physics contain cascade decays. To capture these scenarios, we consider the g_{KK} decay to a pair of top-antitop quarks. Cascade decays can also occur from weakly-produced particles with narrow width. As an example of this scenario we consider Z' bosons decaying to top-antitop pairs in the topcolour model [24]. Finally,

Table 3: Summary of the expected limits for $g_{KK} \to t\bar{t}$ and $Z'_{\text{Topcolor}} \to t\bar{t}$ searches in the lepton+jets (dilepton) channel and of $Z'_{SSM} \to ee$ and $Z'_{SSM} \to \mu\mu$ searches in the Sequential Standard Model for pp collisions at $\sqrt{s}$ = 14 TeV. All boson mass limits are quoted in TeV.

model	300 fb^{-1}	1000 fb^{-1}	3000 fb^{-1}
g_{KK}	4.3 (4.0)	5.6 (4.9)	6.7 (5.6)
$Z'_{\text{Topcolour}}$	3.3 (1.8)	4.5 (2.6)	5.5 (3.2)
$Z'_{SSM} \to ee$	6.5	7.2	7.8
$Z'_{SSM} \to \mu\mu$	6.4	7.1	7.6

one of the simplest and most robust signatures of a new particle is its two-body decay to two leptons, exemplified by $Z' \to ee$ and $Z' \to \mu\mu$ decays [25].

5.1 $t\bar{t}$ resonances

Strongly- and weakly-produced $t\bar{t}$ resonances provide benchmarks not only for cascade decays containing leptons, jets (including b-quark jets) and missing E_T, but also the opportunity to study highly boosted topologies. We study the sensitivity to the KK gluon via the process $pp \to g_{KK} \to t\bar{t}$ in both the dileptonic and the lepton+jets decay modes of the $t\bar{t}$ pair. These decay modes are complementary in a number of ways. The lepton+jets mode allows a more complete reconstruction of the final-state invariant mass which increases the sensitivity of the search. This is particularly true for narrow resonances such as the $Z' \to t\bar{t}$ decay. On the other hand, this mode is more susceptible to W+jets background and to loss of top quark discrimination when the top-jets merge at high boost. This mode also requires b-tagging to suppress a huge light-flavour background. The dominant background for the dilepton channel is Standard Model (SM) $t\bar{t}$ production and b-tagging is not essential for suppressing this background (b-tagging can help suppress diboson and Z+jets backgrounds but these are already insignificant after the Z-mass veto). Finally, the dilepton channel is less susceptible to the merging of top decay products because leptons (especially muons) are easier to identify in close proximity to the b-jet. However the dilepton channel does not allow reconstruction of the resonance mass. By studying both channels we obtain a conservative estimate of the sensitivity from the dilepton channel in comparison to the more sensitive lepton+jets channel.

We have investigated the search sensitivity for different integrated luminosity scenarios. For the dilepton mode, the dominant background is from $t\bar{t}$ production, followed by Z+jets and diboson production. The analysis of current ATLAS data have shown that mis-identification backgrounds from W+jets and QCD multi-jets are not significant. The statistical analysis is performed by constructing templates of the H_T distribution for background plus varying amounts of signal at different resonance masses and cross sections. H_T is defined as the scalar sum of the transverse momenta of the two leading leptons, the two leading jets, and the missing E_T. The likelihood function is defined as the Poisson probability product over all bins for the pseudo-data given the expectation in each bin. The Z+jets and diboson background normalisations are given by the theory cross section, while the $t\bar{t}$ background is floated and is effectively constrained by the low-H_T region. The resulting expected limits in the absence of signal, which we quote as a measure of sensitivity using statistical errors only, are shown in Table 3.

We perform a similar study for the lepton+jets channel where we use the reconstructed $t\bar{t}$ mass spectrum to search for the signal. In this channel we consider the dominant $t\bar{t}$ and W+jets backgrounds; the diboson background is not significant. The sensitivity obtained from the statistical analysis is also shown in Table 3. The distribution of reconstructed resonance mass and the resulting limits as a function of g_{KK} pole mass for the lepton+jets channel are shown in Fig. 8.

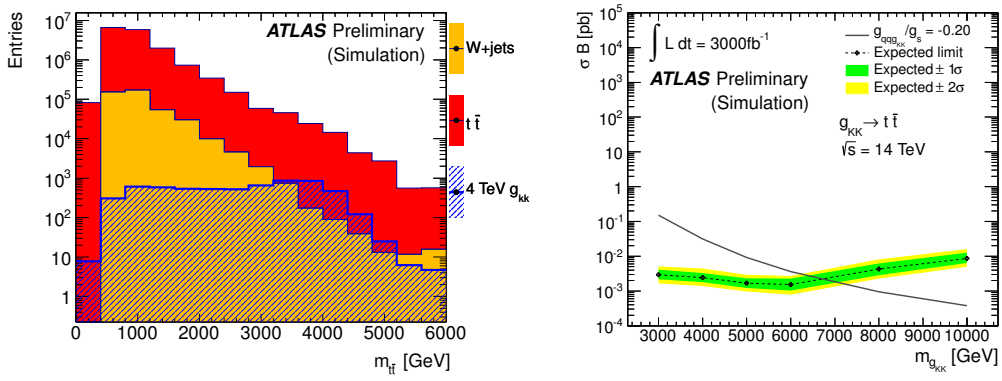

Figure 8: The reconstructed resonance mass spectrum in GeV (left) and limits (right) for the $g_{KK} \to t\bar{t}$ search in the lepton+jets channel with 3000 fb^{-1} for pp collisions at $\sqrt{s} = 14$ TeV.

5.2 Dilepton resonances

The main issues in the detection and reconstruction of very high-p_T electrons and muons from heavy dilepton resonances such as Z' bosons and Randall-Sundrum gravitons are (i) the prevention of EM calorimeter response saturation for electrons due to the readout electronics, (ii) maintaining muon momentum resolution at high p_T, and (iii) maintaining sufficient angular coverage to measure the spin of the resonance. In our sensitivity studies of the Z' boson, we have separated the dielectron and dimuon channels since their momentum resolutions scale differently with p_T and the detector acceptances are different. The sensitivity analysis uses the same methodology that is used for the $t\bar{t}$ study [24] and the Z' search [25] with the current ATLAS data, which is the template-based likelihood fit of the dilepton mass spectrum. The background is dominated by the SM Drell-Yan production, while $t\bar{t}$ and diboson backgrounds are substantially smaller. In the electron channel, there is an additional background from jet-misidentification which needs to be suppressed with good rejection of photon conversions. We assume that the required jet rejection will be achieved with the upgraded detector. The sensitivity study is based on the Drell-Yan background, and the resulting sensitivity is shown in Table 3.

5.3 Summary on exotics

We have shown results of sensitivity studies for a couple of representative exotics signatures, comparing ATLAS datasets of 300 fb^{-1} and 3000 fb^{-1} of integrated luminosity at a pp collision energy of $\sqrt{s} = 14$ TeV. Strongly- and weakly-produced $t\bar{t}$ resonances and narrow dilepton resonances serve as benchmark processes with complex and simple final states respectively. The increase of a factor of ten in integrated luminosity raises the sensitivity to high-mass resonances by up to 2.4 TeV for $t\bar{t}$ resonances and 1.3 TeV for the dilepton Z'_{SSM} resonance.

6 FCNC in top decays

The HL-LHC will provide very large samples of top-quark decays for a programme of precision top physics. Here we consider one example, flavour-changing neutral currents, FCNC.

Although absent at tree level due to the GIM mechanism [26], the FCNC top quark decays occurs in the Standard Model at loop level. The branching ratios are, however, smaller than 10^{-12} [27, 28, 29, 30], many orders of magnitude below the dominant decay mode into bW. There are several Standard Model extensions [31] such as quark-singlet models (QS), two-Higgs doublet (2HDM) and flavour-conserving

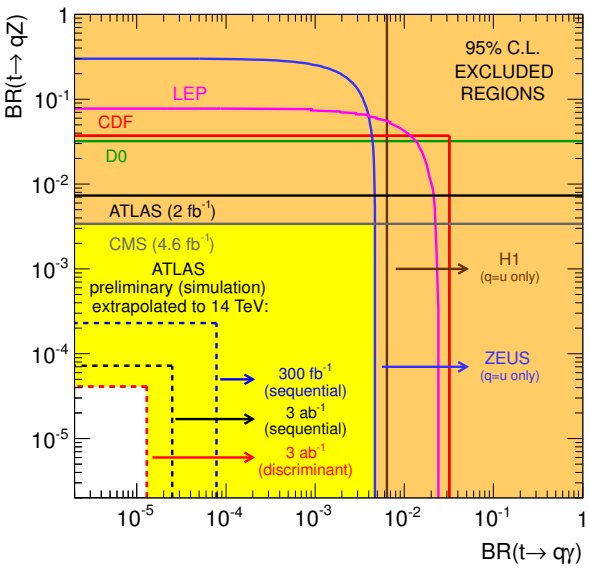

Figure 9: The present 95% CL observed limits on the $BR(t \to q\gamma)$ vs. $BR(t \to qZ)$ plane are shown as full lines for the LEP, ZEUS, H1, D0, CDF, ATLAS and CMS collaborations. The expected sensitivity at ATLAS is also represented by the dashed lines. For an integrated luminosity of $L = 3000\,\text{fb}^{-1}$ the limits range from 1.3×10^{-5} to 2.5×10^{-5} (4.1×10^{-5} to 7.2×10^{-5}) for the $t \to q\gamma$ ($t \to qZ$) decay. Limits at $L = 300\,\text{fb}^{-1}$ are also shown.

two-Higgs doublet (FC 2HDM) models, the minimal supersymmetric (MSSM) model, SUSY with R-parity violation models, the Topcolour-assisted Technicolour model (TC2) [32] as well as models with warped extra dimensions (RS) [33], that significantly enhance the FCNC decay branching ratios, up to 10^{-4}. Here a model independent approach to top quark FCNC decays is performed using an effective Lagrangian [34, 35, 36]. Even if the LHC does not measure the top quark FCNC branching ratios, it can test some of these models or constrain their parameter space, and improve significantly the current experimental limits on the FCNC branching ratios. FCNC top-quark decays have been searched for in the past. The best current direct search limits are 3.2% for $t \to q\gamma$ [37] and 0.34% for $t \to Zq$ ($q = u, c$) [38].

Top quark pair production, in which one of the top quarks decays through the dominant Standard Model channel ($t \to bW$) and the other through a FCNC channel ($t \to q\gamma$, $t \to qZ$), is considered as signal. Several Standard Model processes are background to the present analysis: $t\bar{t}$ production (in which both top quarks decay via Wb), W+jets and Z+jets production, diboson production (WW, WZ and ZZ) and multi-jet production.

The sensitivity is evaluated selecting events as in [39] for the $t \to qZ$ channel and [12] for the $t \to q\gamma$ channel. For the $t \to q\gamma$ channel, the dominant backgrounds are $t\bar{t}$, Z+jets and W+jets events. For the $t \to qZ$ channel, the background is mainly composed of $t\bar{t}$, Z+jets and WZ events.

In the absence of FCNC decays, limits on production cross-sections are estimated and converted to limits on branching ratios using the SM $t\bar{t}$ cross-section. The expected limits at 95% CL for the $t \to q\gamma$ and the $t \to qZ$ channels, are in the range between 10^{-5} and 10^{-4} (10^{-4} and 10^{-3}) for an integrated luminosity of $3000\,\text{fb}^{-1}$ ($300\,\text{fb}^{-1}$). Figure 9 shows the expected sensitivity in the absence of signal, for the $t \to q\gamma$ and $t \to qZ$ channels. Further improvements could come from the use of more sophisticated analysis discriminants.

7 Detector requirements for HL-LHC

The studies discussed in the previous sections show that detector and trigger requirements are similar to those of the present detector. The recent discovery of a 126 GeV Higgs-like resonance makes it particularly important to measure its properties and as many decay modes as possible, requiring triggering on low momentum leptons, measurement of missing transverse momentum and excellent b, τ and forward jet tagging.

The ATLAS detector has been designed for an integrated luminosity of 300 fb^{-1} and a pileup rate of around 20-25 events per bunch crossing. For significantly higher luminosity operation, several upgrades are needed to cope with the higher instantaneous luminosity and the implications of running to much higher integrated luminosity, well beyond the design lifetime of ATLAS. The impact of both the much higher track densities and the integrated radiation levels with 3000 fb^{-1} require the complete replacement of the tracker with a new silicon-only detector. Several improvements are already foreseen this decade to retain low single lepton trigger thresholds given that the LHC performance is projected to already significantly exceed its nominal parameters [40] with particular emphasis on forward muon and calorimeter granularity improvements for Level-1 triggering (Phase-I). The conditions during the high luminosity operation (Phase-II, HL-LHC) require a much more radical approach to retain high selectivity triggering, along with significant further improvements in front-end electronics throughout the experiment, as well as the full tracker replacement. A Letter of Intent explaining the proposed Phase-II upgrades of the detector is in preparation and will show in detail the areas where R&D to build this detector is still needed. The document will be submitted to the LHCC early 2013. The total cost of these upgrades is estimated to be around 280 MCHF. Given the long lead times for such high-technology, complex detectors, R&D and detailed design has been underway for some time with Technical Design Reports required in the coming 2-3 years to be able to establish funding and meet the proposed construction schedules.

8 Conclusions

Studies illustrating the physics case of a luminosity upgrade of the LHC have been presented. In general, a substantial gain in the physics reach is possible with 3000 fb^{-1}, and some studies are only viable with this high integrated luminosity. The precision on the production cross section times branching ratio for most Higgs decay modes can be improved by a factor two to three. Furthermore the rare decay mode of the Higgs boson $H \to \mu\mu$ only becomes accessible with 3000 fb^{-1}. Combining both experiments, first evidence for the Higgs self-coupling, and thus a proof that the Higgs mechanism works as predicted, may be within reach. In searches for new particles, the mass reach can be increased by up to 50%.

The luminosity upgrade would become even more interesting if new phenomena are seen during the 300 fb^{-1} phase of the LHC, as the ten-fold increase in luminosity would give access to measurements of the new physics.

To reach these goals a detector performance similar to that of the present one is needed, however under much harsher pileup and radiation conditions than today. The ATLAS Collaboration strongly supports the high-luminosity operation with the goal of an integrated luminosity of 3000 fb^{-1}.

References

[1] ATLAS Collaboration, arXiv:1207.7214 [hep-ex].

[2] CMS Collaboration, arXiv:1207.7235 [hep-ex].

[3] F. Gianotti et al., arXiv:0204087 [hep-ph].

[4] ATLAS Collaboration, arXiv:1206.5971 [hep-ex].

[5] ATLAS Collaboration, ATLAS-CONF-2012-094.
https://cdsweb.cern.ch/record/1460440.

[6] HPAIR package: http://people.web.psi.ch/spira/proglist.html.

[7] M. J. Dolan, C. Englert, and M. Spannowsky, arXiv:1206.5001 [hep-ph].

[8] U. Baur, T. Plehn, and D. L. Rainwater, Phys.Rev. **D69** (2004) 053004, arXiv:hep-ph/0310056 [hep-ph].

[9] A. Dobado, M. Herrero, J. Pelaez, and E. Ruiz Morales, Phys. Rev. **D62** (2000) 055011, arXiv:hep-ph/9912224 [hep-ph]. (and references therein).

[10] A. Alboteanu, W. Kilian, and J. Reuter, arXiv:0806.4145 [hep-ph].

[11] M. Beyer et al., Eur. Phys. J. **C48** (2006) 353–388, arXiv:0604048 [hep-ph].

[12] ATLAS Collaboration, arXiv:0901.0512 [hep-ex].

[13] J. Butterworth, B. E. Cox, and J. R. Forshaw, arXiv:0201098 [hep-ph].

[14] ATLAS Collaboration, arXiv:1208.0949 [hep-ex].

[15] ATLAS Collaboration, ATLAS-CONF-2012-073.
https://cdsweb.cern.ch/record/1460270.

[16] ATLAS Collaboration, ATLAS-CONF-2012-077.
https://cdsweb.cern.ch/record/1460274.

[17] ATLAS Collaboration, ATLAS-CONF-2012-076.
https://cdsweb.cern.ch/record/1460273.

[18] W. Beenakker, R. Hopker, M. Spira, and P. Zerwas, Nucl.Phys. **B492** (1997) 51–103, arXiv:hep-ph/9610490 [hep-ph].

[19] H. Baer, V. Barger, A. Lessa, and X. Tata, arXiv:1207.4846 [hep-ph].

[20] R. Barbieri and G. Giudice, Nucl.Phys. **B306** (1988) 63.

[21] B. de Carlos and J. Casas, Phys.Lett. **B309** (1993) 320–328, arXiv:hep-ph/9303291 [hep-ph].

[22] C. Lester and D. Summers, Phys.Lett. **B463** (1999) 99–103, arXiv:hep-ph/9906349 [hep-ph].

[23] A. Barr, C. Lester, and P. Stephens, J.Phys.G **G29** (2003) 2343–2363, arXiv:hep-ph/0304226 [hep-ph].

[24] ATLAS Collaboration, arXiv:1205.5371 [hep-ex]. (and references therein).

[25] ATLAS Collaboration, Phys. Rev. Lett. **107** (2011) 272002. (and references therein).

[26] S. L. Glashow, J. Iliopoulos, and L. Maiani, Phys. Rev. **D2** (1970) 1285–1292.

[27] J. L. Diaz-Cruz, R. Martinez, M. A. Perez, and A. Rosado, Phys. Rev. **D41** (1990) 891–894.

[28] G. Eilam, J. L. Hewett, and A. Soni, Phys. Rev. **D44** (1991) 1473–1484. Erratum-ibid.D59:039901,1999.

[29] B. Mele, S. Petrarca, and A. Soddu, Phys. Lett. **B435** (1998) 401–406, arXiv:hep-ph/9805498.

[30] J. A. Aguilar-Saavedra and B. M. Nobre, Phys. Lett. **B553** (2003) 251–260, arXiv:hep-ph/0210360.

[31] J. A. Aguilar-Saavedra, Acta Phys. Polon. **B35** (2004) 2695–2710, arXiv:hep-ph/0409342.

[32] G. Lu, F. Yin, X. Wang, and L. Wan, Phys. Rev. **D68** (2003) 015002, arXiv:hep-ph/0303122.

[33] G. P. K. Agashe and A. Soni, Phys. Rev. D **75** (2007) 015002, arXiv:hep-ph/0606293.

[34] C. Caso et al., Eur. Phys. J. C **3** (1998) 1.

[35] W. Hollik, J. I. Illana, S. Rigolin, C. Schappacher and D. Stockinger, Nucl. Phys. B **551** (1999) 3.

[36] M. Beneke et al., arXiv:hep-ph/0003033.

[37] CDF Collaboration, F. Abe et al., Phys. Rev. Lett. **80** (1998) 2525–2530.

[38] CMS Collaboration, CMS PAS-TOP-11-028 .

[39] ATLAS Collaboration, arXiv:1206.0257 [hep-ex].

[40] ATLAS Collaboration, *ATLAS Letter of Intent Phase-I Upgrade*, LHCC-I-20.